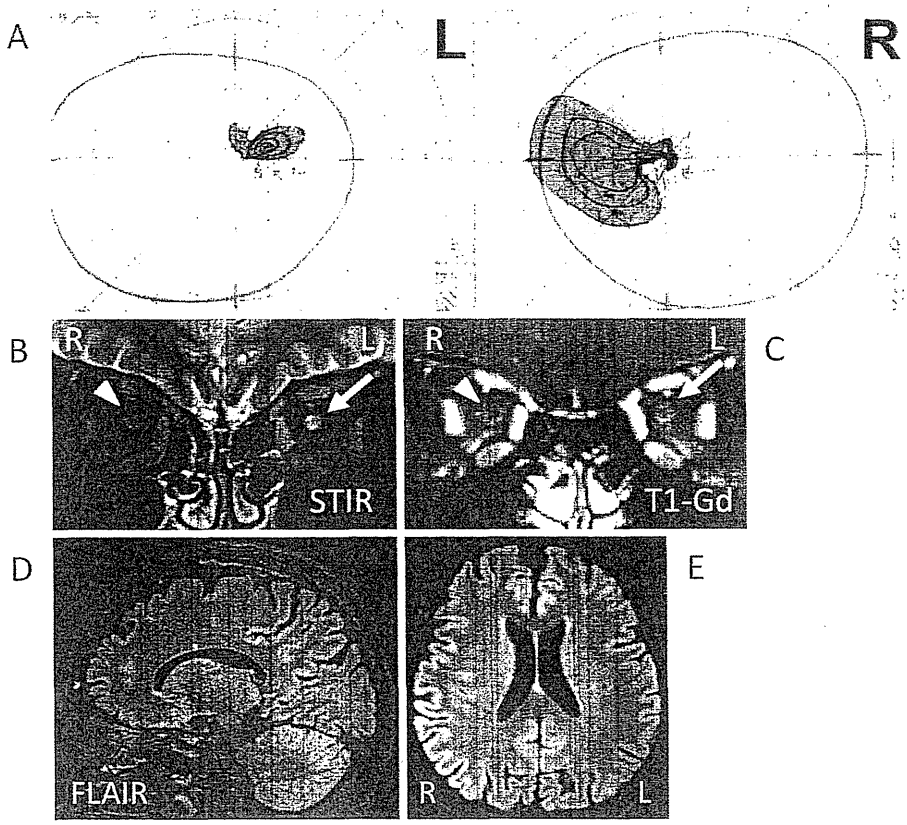

Figure 2. The visual impairment and the magnetic resonance images of the present case. The Goldmann visual fields on admission are highlighted (A). The left optic nerve showed high signal intensity on the STIR coronal image (white arrow, B) with marginal contrast enhancement (white arrow, C). The right optic nerve showed no remarkable findings (arrow head, B and C). The brain showed no particular findings except for the optic nerve on FLAIR saggital (D) and axial (E) images. FLAIR: fluid-attenuated inversion recovery, STIR: short inversion time inversion-recovery, T1-Gd: gadolinium enhanced T1

noglobulin (400 mg/kg/day for five days), and high-dose cyclophosphamide (CPM) (500 mg/day for one day). The exacerbation of the visual impairment was halted by this treatment. In September 2011, the patient was discharged from our hospital with a plan to undergo monthly CPM therapy.

Discussion

The present patient developed T1DM during IFN-α therapy and anti-AQP4 antibody positive optic neuritis after IFN-β, followed by IFN-α, therapy. Her severe visual impairment persisted despite the use of intensive immunotherapy. Several reasons for the intractable disease course can be proposed. For example, the type 1 IFNs or HCV infection may have served as a potent activator of autoimmunity, or the involvement of vasculitis as an extrahepatic manifestation of HCV infection (2) could lead to the clinical deterioration.

The first case of T1DM development during IFN-α therapy for chronic hepatitis C was reported in 1992 (3). New-onset DM among IFN-treated patients has been documented to occur in 0.7% of patients in Japan (4). The mechanism underlying immune-mediated pancreatic β-cell destruction can be attributed to genetic and environmental causes thus leading to the generation of islet cell autoantibodies, i.e., anti-GAD autoantibodies. IFN-α may act as an initiator of the autoimmunity directed against β cells, thus leading to the pathogenesis of T1DM. Likewise, IFN-α can be considered to play a critical role in the pathogenesis of systemic lupus erythematosus.

To date, ten cases of new-onset optic neuritis, multiple sclerosis (MS), MS-like disease, or NMOsd associated with IFN-α therapy for chronic viral hepatitis or malignant neoplasms, have been reported (5-11). There were two cases with seropositivity for anti-AQP4 antibodies (Table); one patient with optic-spinal MS (OSMS) after IFN-α2b and RBV (10), and another patient with NMOsd after PEG-IFN-α and RBV (11). In the remaining eight cases, the presence of anti-AQP-4 antibodies was not examined because they had been reported before the discovery of NMO-Immunoglobulin G (IgG) and anti-AQP-4 (12) antibodies.

IFN-β therapy can also play a role as an initiator of autoimmune diseases involving the central nervous system. A case with new-onset optic neuritis after IFN-β therapy for

Table. The Reported Cases of Newly-onset Anti-AQP-4 Antibody Positive OSMS, and NMOsd Provoked by Type 1 IFN Therapy

Patient age, sex	Disease	IFN	ON	SC	B	AQP4-Ab	Duration	References
47, F	Hepatitis C	α-2b/RBV	+	+	+	+	1Y	Kajiyama, et al. 2007[10]
65, F	Hepatitis C	α/RBV	+	-	+	+	2Y10M	Yamasaki, et al. 2012[11]
60, F	Hepatitis C	α, β, α/RBV	+	-	-	+	α: 15Y β: 9M	Present Case 2012

RBV: ribavirin, ON: optic neuritis, SC: spinal cord lesion, B: brain lesion. Duration: duration between the initiation of type I IFN therapy and the onset of OSMS or NMOsd

kidney cancer has been reported (13). In addition, a number of exacerbated cases of relapsing-remitting MS (RRMS) have been reported in Japan in patients receiving IFN-β (14). Differentiating between NMO and MS can be achieved based on seropositivity for the anti-AQP-4 antibodies, longitudinally extensive spinal cord lesions, and brain MRI findings not meeting the diagnostic criteria for MS (15). However, before the discovery of this autoantibody, it was difficult to distinguish NMO from MS, especially OSMS, which is common in Asian countries. In 2000, IFN-β therapy was approved in Japan for the prevention of relapse and progression of RRMS, in which patients with OSMS were also included. Consequently, exacerbation of the disease or ineffectiveness of IFN-β was reported among patients with OSMS who underwent IFN-β therapy (14, 16). These cases were later found to be positive for anti-AQP-4 antibodies. Recent articles described that IFN-β treatment was not effective in preventing relapses in NMO patients (17, 18), while strictly defined OSMS showed a response to IFN-β treatment in terms of the prevention of relapses and functional worsening (19).

The mechanism underlying the onset and exacerbation of NMO/NMOsd has not been well understood, but the induction of B-cell activation factors of the tumor necrosis factor (TNF) family by IFN-β is considered to facilitate the production of anti-AQP-4 antibodies (20). For example, Chihara et al. have shown that IL-6-dependent B-cell subpopulations of plasmablasts are involved in the production of anti-AQP-4 antibodies (21). Loss of AQP-4, mediated by immunoglobulins and complements, has been shown in inflammatory lesions of patients with NMO (22). These results indicate that the anti-AQP-4 antibody plays a crucial role in the pathogenesis of NMO, unlike in cases of MS. As another mechanism underlying the development of type 1 IFN-induced NMO/NMOsd, it has been suggested that IFN-β treatment leads to the overproduction of IL-17 from T helper 17 (Th17) cells (23), which is thought to be associated with the pathological feature of NMO.

Type 1 IFN has reciprocal characteristics, with both pathogenic and protective roles in autoimmunity. In general, IFN-β exerts its therapeutic effect on MS by producing anti-inflammatory cytokines and suppressing the proliferation of autoreactive T cells. Both IFN-α and IFN-β bind to a single heterodimeric receptor composed of IFNAR1 and IFNAR2, which can cause similar immunomodulatory effects (24). Hence, it is likely that IFN-α has a similar effect on autoimmunity as does IFN-β, as indicated by the fact that IFN-α has also been developed as a candidate therapeutic agent for MS (25).

Type 1 IFNs served as pathogenic mediators in the present case, inducing T1DM and NMO/NMOsd. Since various types of IFN-α treatment had been carried out intermittently for more than ten years after the onset of chronic hepatitis C, the onset of T1DM was clearly influenced by IFN-α treatment. However, it remains unclear which type of IFN was involved in the induction of NMOsd. We speculate that the combination therapy with IFN-α and IFN-β may have produced synergistic effects to trigger NMOsd in the present case.

The authors state that they have no Conflict of Interest (COI).

Acknowledgement

We thank Dr. Toshiyuki Takahashi from the Department of Neurology and Multiple Sclerosis Therapeutics, Tohoku University Graduate School of Medicine, for measuring the titer of anti-AQP-4 antibodies. We also thank Dr. Motoki Takashima and Dr. Akihisa Miyazaki from the Department of Gastroenterology, Juntendo University Nerima Hospital, for providing the medical information on hepatitis C.

Contributor TK, MA, and MW undertook the clinical management of the patient. MW referred the patient to NCNP and performed the ophthalmological examination. Each of the authors was significantly involved in clinical assessments of the patient.

TK and MA equally contributed to this work.

References

1. Burdick LM, Somani N, Somani AK. Type I IFNs and their role in the development of autoimmune diseases. Expert Opin Drug Saf 8: 459-472, 2009.
2. Cacoub P, Poynard T, Ghillani P, et al. Extrahepatic manifestations of chronic hepatitis C. Arthritis Rheum 42: 2204-2212, 1999.
3. Fabris P, Betterle C, Floreani A, et al. Development of type 1 dia-

betes mellitus during interferon alfa therapy for chronic HCV hepatitis. Lancet **340**: 548, 1992.
4. Okanoue T, Sakamoto S, Itoh Y, et al. Side effects of high-dose interferon therapy for chronic hepatitis C. J Hepatol **25**: 283-291, 1996.
5. Manesis EK, Petrou C, Brouzas D, Hadziyannis S. Optic tract neuropathy complicating low-dose interferon treatment. J Hepatol **21**: 474-477, 1994.
6. Isler M, Akhan G, Bardak Y, Akkaya A. Dry cough and optic neuritis: two rare complications of interferon alpha treatment in chronic viral hepatitis. Am J Gastroenterol **96**: 1303-1304, 2001.
7. Matsuo T, Takabatake R. Multiple sclerosis-like disease secondary to alpha interferon. Ocul Immunol Inflamm **10**: 299-304, 2002.
8. Kataoka I, Shinagawa K, Shiro Y, et al. Multiple sclerosis associated with interferon-alpha therapy for chronic myelogenous leukemia. Am J Hematol **70**: 149-153, 2002.
9. Höftberger R, Garzuly F, Dienes HP, et al. Fulminant central nervous system demyelination associated with interferon-alpha therapy and hepatitis C virus infection. Mult Scler **13**: 1100-1106, 2007.
10. Kajiyama K, Tsuda K, Takeda M, Yoshikawa H, Tanaka K. Multiple sclerosis with positive anti-aquaporin-4 antibody, manifested after interferon-a-2b/ribavirin therapy for chronic hepatitis C. A case report. Shinkeinaika (Neurol Med) **66**: 180-184, 2007 (in Japanese, Abstract in English).
11. Yamasaki M, Matsumoto K, Takahashi Y, Nakanishi H, Kawai Y, Miyamura M. A case of NMO (Neuromyelitis optica) spectrum disorder triggered by interferon alpha, which involved extensively pyramidal tract lesion of the brain. Rinshou Shinkeigaku (Clin Neurol) **52**: 19-24, 2012.
12. Lennon VA, Wingerchuk DM, Kryzer TJ, et al. A serum autoantibody marker of neuromyelitis optica: distinction from multiple sclerosis. Lancet **364**: 2106-2112, 2004.
13. Okuma H, Kawamura Y, Ohnuki Y, Takagi S. Optic neuritis caused by interferon-beta administration. Intern Med **47**: 1759, 2008.
14. Shimizu J, Hatanaka Y, Hasegawa M, et al. IFNβ-1b may severely exacerbate Japanese optic-spinal MS in neuromyelitis optica spectrum. Neurology **75**: 1423-1427, 2010.
15. Wingerchuk DM, Lennon VA, Pittock SJ, Lucchinetti CF, Weinshenker BG. Revised diagnostic criteria for neuromyelitis optica. Neurology **66**: 1485-1489, 2006.
16. Matsuoka T, Matsushita T, Kawano Y, et al. Heterogeneity of aquaporin-4 autoimmunity and spinal cord lesions in multiple sclerosis in Japanese. Brain **130**: 1206-1223, 2007.
17. Tanaka M, Tanaka K, Komori M. Interferon-beta(1b) treatment in neuromyelitis optica. Eur Neurol **62**: 167-170, 2009.
18. Uzawa A, Mori M, Hayakawa S, Masuda S, Kuwabara S. Different responses to interferon beta-1b treatment in patients with neuromyelitis optica and multiple sclerosis. Eur J Neurol **17**: 672-676, 2010.
19. Shimizu Y, Fujihara K, Kubo S, et al. Therapeutic efficacy of interferon b-1b in Japanese patients with optic-spinal multiple sclerosis. Tohoku J Exp Med **223**: 211-214, 2011.
20. Krumbholz M, Faber H, Steinmeyer F, et al. Interferon-beta increases BAFF levels in multiple sclerosis: implications for B cell autoimmunity. Brain **131**: 1455-1463, 2008.
21. Chihara N, Aranami T, Sato W, et al. Interleukin 6 signaling promotes anti-aquaporin 4 autoantibody production from plasmablasts in neuromyelitis optica. Proc Natl Acad Sci U S A **108**: 3701-3706, 2011.
22. Misu T, Fujihara K, Kakita A, et al. Loss of aquaporin 4 in lesions of neuromyelitis optica: distinction from multiple sclerosis. Brain **130**: 1224-1234, 2007.
23. Axtell RC, Raman C, Steinman L. Interferon-b exacerbates Th17-mediated inflammatory disease. Trends Immunol **32**: 272-277, 2011.
24. Crow MK. Type 1 interferon in organ-targeted autoimmune and inflammatory diseases. Arthritis Res Ther **12**(Suppl 1): S5-S14, 2010.
25. Knobler RL, Panitch HS, Braheny SL, et al. Systemic alpha-interferon therapy of multiple sclerosis. Neurology **34**: 1273-1279, 1984.

Journal of the Neurological Sciences xxx (2012) xxx–xxx

Contents lists available at SciVerse ScienceDirect

Journal of the Neurological Sciences

journal homepage: www.elsevier.com/locate/jns

Heterozygous UDP-GlcNAc 2-epimerase and *N*-acetylmannosamine kinase domain mutations in the *GNE* gene result in a less severe GNE myopathy phenotype compared to homozygous *N*-acetylmannosamine kinase domain mutations

Madoka Mori-Yoshimura [a,*], Kazunari Monma [b], Naoki Suzuki [c], Masashi Aoki [c], Toshihide Kumamoto [d], Keiko Tanaka [e], Hiroyuki Tomimitsu [f], Satoshi Nakano [g], Masahiro Sonoo [h], Jun Shimizu [i], Kazuma Sugie [j], Harumasa Nakamura [a,k], Yasushi Oya [a], Yukiko K. Hayashi [b], May Christine V. Malicdan [b], Satoru Noguchi [b], Miho Murata [a], Ichizo Nishino [b]

[a] *Department of Neurology, National Center Hospital, National Center of Neurology and Psychiatry, 4-1-1 Ogawahigashi, Kodaira, Tokyo 187-8551, Japan*
[b] *Department of Neuromuscular Research, National Institute of Neuroscience, National Center of Neurology and Psychiatry, 4-1-1 Ogawahigashi, Kodaira, Tokyo 187-8502, Japan*
[c] *Department of Neurology, Tohoku University School of Medicine, 1-1 Seiryo, Aoba-ku, Sendai 980-8574, Japan*
[d] *Department of Internal Medicine 3, Faculty of Medicine, Oita University, 1-1 Idaigaoka, Hasama, Yufu-shi, Oita 879-5593, Japan*
[e] *Department of Neurology, Kanazawa Medical University, 1-1 Daigaku, Uchinadamachi, Kahoku-gun, Ishikawa, 920-0214, Japan*
[f] *Department of Neurology and Neurological Science, Graduate School, Tokyo Medical and Dental University, Yushima 1-5-45, Bunkyo-ku, Tokyo 113-8519, Japan*
[g] *Department of Neurology, Osaka City General Hospital, 2-13-22, Miyakojimahonndoori, Miyakojima-ku, Osaka534-0021, Japan*
[h] *Department of Neurology, Teikyo University School of Medicine, Kaga 2-11-1, Itabashi-ku, Tokyo 173-8605, Japan*
[i] *Department of Neurology, Division of Neuroscience, Graduate School of Medicine, University of Tokyo, 7-3-1 Hongo, Bunkyo-ku, Tokyo 113-8655, Japan*
[j] *Department of Neurology, Nara Medical University School of Medicine, 840 Shijo, Kashihara, Nara 634-8521, Japan*
[k] *Clinical Trial Division, Division of Clinical Research, National Center Hospital of Neurology and Psychiatry, 4-1-1 Ogawahigashi, Kodaira, Tokyo 187-8551, Japan*

ARTICLE INFO

Article history:
Received 10 January 2012
Received in revised form 20 March 2012
Accepted 21 March 2012
Available online xxxx

Keywords:
GNE myopathy
Distal myopathy with rimmed vacuoles
Hereditary inclusion body myopathy
Glucosamine (UDP-N-acetyl)-2-epimerase/
N-acetylmannosamine kinase
(UDP-N-acetyl)-2-epimerase domain
N-acetylmannosamine kinase domain
Questionnaire
Natural history

ABSTRACT

Background: Glucosamine (UDP-N-acetyl)-2-epimerase/*N*-acetylmannosamine kinase (GNE) myopathy, also called distal myopathy with rimmed vacuoles (DMRV) or hereditary inclusion body myopathy (HIBM), is a rare, progressive autosomal recessive disorder caused by mutations in the *GNE* gene. Here, we examined the relationship between genotype and clinical phenotype in participants with GNE myopathy.
Methods: Participants with GNE myopathy were asked to complete a questionnaire regarding medical history and current symptoms.
Results: A total of 71 participants with genetically confirmed GNE myopathy (27 males and 44 females; mean age, 43.1 ± 13.0 (mean ± SD) years) completed the questionnaire. Initial symptoms (*e.g.*, foot drop and lower limb weakness) appeared at a mean age of 24.8 ± 8.3 years. Among the 71 participants, 11 (15.5%) had the ability to walk, with a median time to loss of ambulation of 17.0 ± 2.1 years after disease onset. Participants with a homozygous mutation (p.V572L) in the *N*-acetylmannosamine kinase domain (KD/KD participants) had an earlier disease onset compared to compound heterozygous participants with mutations in the uridine diphosphate-N-acetylglucosamine (UDP-GlcNAc) 2-epimerase and *N*-acetylmannosamine kinase domains (ED/KD participants; 26.3 ± 7.3 vs. 21.2 ± 11.1 years, respectively). KD/KD participants were more frequently non-ambulatory compared to ED/KD participants at the time of survey (80% vs. 50%). Data were verified using medical records available from 17 outpatient participants.
Conclusions: Homozygous KD/KD participants exhibited a more severe phenotype compared to heterozygous ED/KD participants.

1. Introduction

Glucosamine (UDP-N-acetyl)-2-epimerase/*N*-acetylmannosamine kinase (GNE) myopathy, also known as distal myopathy with rimmed vacuoles (DMRV), Nonaka myopathy (MIM: 605820) or hereditary inclusion body myopathy (HIBM; MIM: 600737), is an early adult-onset, progressive myopathy that affects the tibialis anterior muscle, but spares quadriceps femoris muscles [1,2]. The disease is caused by a mutation in the *GNE* gene, which encodes a bifunctional enzyme [uridine diphosphate-*N*-acetylglucosamine (UDP-GlcNAc) 2-epimerase (GNE) and *N*-acetylmannosamine kinase (MNK)] known to catalyze two rate-limiting reactions involved in cytosolic sialic acid synthesis [3–7]. Mutations in the *GNE* gene result in decreased enzymatic activity *in vitro* by 30–90% [7–10]. Therefore, hyposialylation is thought to

* Corresponding author. Tel.: +81 42 341 2711; fax: +81 42 346 1852.
E-mail address: yoshimur@ncnp.go.jp (M. Mori-Yoshimura).

0022-510X/$ – see front matter © 2012 Elsevier B.V. All rights reserved.
doi:10.1016/j.jns.2012.03.016

contribute to the pathogenesis of GNE myopathy. This is supported by the myopathic phenotype associated with a mouse model expressing the human D176V mutant GNE protein (GNE−/−hGNED176V-Tg) [11]. Muscle atrophy and weakness are prevented by oral treatment with sialic acid metabolites in this mouse model [12].

A phase I clinical trial using oral sialic acid therapy has recently been performed in Japan for the treatment of GNE myopathy (ClinicalTrials.gov; NCT01236898). A similar phase I study is currently underway in the United States (ClinicalTrials.gov; NCT01359319). Natural history and genotype–phenotype correlations need to be established for a successful phase II clinical trial for the treatment of GNE myopathy. However, only a small number of studies have been conducted that review the natural course of this disease. In addition, the presence of genotype–phenotype correlations is controversial in GNE myopathy, with most reports denying significant correlations [7]. In fact, substantial heterogeneity is observed among participants who have the same mutations. For example, few subjects with p.D176V and p.M712T mutations exhibited a normal or very mild phenotype, with disease onset after the age of 60 [3,13]. Furthermore, only a limited number of studies that analyze compound heterozygous patients are available. Nonetheless, such studies report a variable degree of severity [14–17].

To clarify the potential relationship between genotype and clinical phenotype (*i.e.*, age at onset, disease course, and current symptoms) of GNE myopathy, we performed a questionnaire-based survey of participants with confirmed GNE myopathy.

2. Participants and methods

2.1. Study population

We obtained approval for this study from the Medical Ethics Committee of the National Center of Neurology and Psychiatry (NCNP). Seventy-eight participants with known GNE myopathy were seen at 8 hospitals specializing in muscle disorders in Japan and 83 participants (not all genetically diagnosed) from the Participants Association for Distal Myopathies (PADM) were recruited. Participants provided written informed consent prior to completing the questionnaire.

A total of 75 participants completed and returned the questionnaire. Of the 75 participants analyzed, 4 were found to have only one heterozygous mutation. Because single heterozygous mutations have not been confirmed to cause GNE myopathy, these 4 participants were excluded from this study.

2.2. Study design

The present study is a retrospective and cross-sectional analysis, which includes 71 participants with genetically confirmed GNE myopathy. Clinical information was collected from participants using a questionnaire and genetic information was acquired from available medical records.

2.3. Questionnaire

Participants completed a self-reporting questionnaire regarding 1) developmental and past symptoms, 2) past and present ambulatory status, and 3) information about diagnosis and medical services (Supplementary material, original version in Japanese).

To determine developmental history, we collected the following information: 1) trouble before and/or during delivery, 2) body weight and height at birth, 3) age at first gait, 4) exercise performance during nursery, kindergarten, or school, and 5) age at onset and signs of first symptoms. Participants were also asked about the onset of 1) gait disturbance, 2) walking with assistance (*i.e.*, cane and/or orthotics and/or handrails), 3) wheelchair use, 4) loss of ambulation, and 5) current gait performance. With regard to medical history, participants were asked about 1) age at the time of first hospital visit, 2) whether or not they had symptoms at the time of visit, 3) age at the time of final diagnosis, 4) how many hospitals/clinics were visited before final diagnosis, and 5) whether a biopsy was performed.

2.4. Medical record examination

To verify the accuracy of the information provided by each participant, available medical records from 17 participants (23.9%) seen at outpatient clinics at NCNP were examined (9 males and 8 females).

2.5. Data handling and analysis

All variables were summarized using descriptive statistics, which included mean, standard deviation (SD), median, range, frequency, and percentage. Each variable was compared against age, sex, genotype, and domain mutation (*i.e.*, within the UDP-GlcNAc 2-epimerase domain: ED or *N*-acetylmannosamine kinase domain: KD). Student's *t* test was used to compare the means for each participant group (ED/ED, ED/KD and KD/KD participants). Data from the two participant groups were calculated using chi-square contingency table analysis. The time from disease onset to walking with assistance, time from disease onset to wheelchair use, and time from disease onset to loss of ambulation were evaluated using the Kaplan–Meier method with log-rank analysis. Questionnaire reliability was tested using intraclass correlation coefficients (ICCs), and two-sided 95% confidence intervals (CIs) were calculated using a one-way random effects analysis of variance model for inter-rater reliability. All analyses were performed using SPSS for Macintosh (version 18, SPSS Inc., Chicago, IL).

3. Results

3.1. General characteristics

A total of 71 Japanese individuals (27 males and 44 females) participated in the study. The mean age at data collection was 43.1 ± 10.7 years. None of the participants showed developmental abnormalities during infancy or early childhood.

3.2. GNE mutations

Forty-one percent of study participants (n = 29/71) had homozygous mutations, while 59% (n = 42/71) had compound heterozygous mutations (Table 1). Among homozygous participants, 86.2% (n = 25/29) harbored the p.V572L mutation, while the remaining participants had other mutations. No homozygous participants for the p.D176V mutation were identified. Among compound heterozygous participants, 28.5% (n = 12/42) had p.D176V/p.V572L mutations, while the remaining participants had other mutations. With respect to allelic frequency, 50.0% (71/142) were p.V572L, 20.4% (29/142) p.D176V, 3.5% (5/142) p.C13S, 2.8% (4/142) p.M712T, and 2.1% (3/142) p.A630T. All other mutations accounted for 2%. A total of 18.3% (n = 13/71) of participants were homozygous with a mutation in the GNE domain (ED/ED), 39.4% (n = 28/71) of participants were compound heterozygous with a mutation in the GNE domain and one in the MNK domain (ED/KD), and 42.3% (n = 30/71) of participants had a mutation in the MNK domain in both alleles (KD/KD).

3.3. Past and present symptoms

Mean participant age at symptom onset was 25.2 ± 9.2 years (range, 12–58 years; median, 24.5 years). There was no significant difference between males and females for current age, age at disease

Please cite this article as: Mori-Yoshimura M, et al. Heterozygous UDP-GlcNAc 2-epimerase and *N*-acetylmannosamine kinase domain mutations in the *GNE*... J Neurol Sci (2012), doi:10.1016/j.jns.2012.03.016

Table 1
Genotypes of the GNE myopathy patient population.

		Questionnaire	Outpatients
ED/ED	Total	13	4
	Homozygote	1	0
	p.C13S homozygote	1	
	Compound heterozygote	12	4
	p.C13S/p.M29T	1	1
	p.C13S/p.A63I	1	1
	p.D176V/p.F233S	1	1
	p.D176V/p.R306Q	2	
	p.R129Q/p.D176V	1	
	p.R129Q/p.R277C	1	
	p.D27L/p.D176V	1	1
	p.B89S/p.D176V	1	
	p.D176V/p.R246W	1	
	p.D176V/p.R321C	1	
	p.D176V/p.V331A	1	
ED/KD	Total	28	8
	Compound heterozygote	28	8
	p.D176V/p.V572L	12	3
	p.C13S/p.V572L	1	1
	p.D176V/p.I472T	1	1
	p.D176V/p.L603F	1	1
	p.R177C/p.V572L	1	1
	383insT/p.V572L	1	1
	p.D176V/p.G708S	2	
	p.D187G/p.V572L	2	
	p.R8X/p.V572L	1	
	p.D176V/p.G568S	1	
	p.D176V/p.H626R	1	
	p.D176V/p.A630T	1	
	p.I276T/p.V572L	1	
	p.G295D/p.A631V	1	
	p.A600E/p.D176V	1	
KD/KD	Total	30	5
	Homozygote	28	5
	p.V572L homozygote	25	4
	p.M712T homozygote	2	
	p.A630T homozygote	1	
	Compound heterozygote	2	0
	p.V572L/p.R420X	1	1
	1756Gdel (stop)/p.V572L	1	

onset, age at walking with assistance, age at wheelchair use, and current ambulatory status. Initial symptoms included gait disturbance (66.2%, n = 47/71), other lower limb symptoms (26.8%, n = 19/71), easily fatigued (23.9%, n = 17/71), and weakness of hands and fingers (8.5%, n = 6/71). In addition, 21.1% (n = 15/71) had onset of symptoms before the age of 20. When specifically asked, 47.8% (n = 34/71) described themselves as slow runners during childhood, and 42.5% reported having had difficulty with physical exercise during school years.

3.4. Diagnosis

Mean participant age at diagnosis was 33.9 ± 12.6 years (median, 29.5 years; range 17 to 67 years). Mean participant age at first physician visit was 29.6 ± 10.4 years (median, 27 years; range, 12–62 years), and mean time between first visit and diagnosis was 4.4 ± 8.3 years.

3.5. Walking with assistance and wheelchair use

At the time of the survey, 52.0% (n = 37/71) were ambulant (41.3 ± 12.8 years); however, only 15.5% (n = 11/71, 40.0 ± 13.6 years) could walk without assistance, with the remaining 35.2% requiring assistance (n = 25/71, 41.8 ± 12.7 years). Only 7.0% of these participants (n = 5/71) could walk up stairs, while 49.3% (n = 35/71) were non-ambulant. Wheelchairs were used by 63.6% (23.9% partially bound and 43.7% totally bound) and an electric wheelchair was used by 41.9% (n = 31/71). Mean participant age of wheelchair users was 34.9 ± 11.7 years (range, 18–70 years). Wheelchairs were not used by 32.4% (n = 26/71) of participants. Current age of wheelchair-free participants was 39.4 ± 12.3 years (range, 21–61 years; median, 34 years) and that of wheelchair-bound participants was 42.8 ± 12.6 years (range, 21–71; median, 42 years).

Kaplan–Meier analysis revealed a median proportional age at walking with assistance of 30.0 ± 1.4 years. Median proportional age of wheelchair users was 36.0 ± 2.7 years, and that for loss of ambulation was 45.0 ± 4.2 years. The time from disease onset to walking with assistance was 7.0 ± 0.4 years, time from disease onset to wheelchair use was 11.5 ± 1.2 years, and time from disease onset to loss of ambulation was 17.0 ± 2.1 years.

3.6. Correlation between disease genotype and phenotype

To determine if a correlation between genotype and phenotype existed, we compared domain mutations (ED/KD, or both) available from medical reports to questionnaire answers (Table 2). Participants with KD/KD mutations (both homozygous and heterozygous) were younger and more severely affected compared to participants with ED/KD or ED/ED mutations. No significant difference in current age or age at disease onset between ED/ED and ED/KD participants was identified. Kaplan–Meier analyses revealed that the proportional time from disease onset to wheelchair use and from disease onset to loss of ambulation was significantly shorter in KD/KD compared to ED/KD participants. ED/ED participants exhibited a shorter time of disease onset to wheelchair use compared to ED/KD participants (Table 3, Fig. 1).

3.7. Comparison between p.V572L homozygous and p.D176V/p.V572L compound heterozygous participants

To compare clinical features in patients with the same mutations, we specifically analyzed data from those with p.V572L (n = 25/71, 35.2%) and p.D176V/p.V572L (n = 12/71, 16.9%) mutations, as these two were the most frequent mutations in our study population (Table 2). Age at disease onset of homozygous participants (p.V572L) was 21.3 ± 5.7 years (range, 12–32 years) and time from disease onset to wheelchair use was 11.3 ± 5.4 years (range, 3–21 years). Only 16.0% (n = 4/25) of these homozygous participants reported that they were not currently using a wheelchair. In contrast, the mean age at disease onset of heterozygous participants (p.D176V/p.V572L) was 35.5 ± 14.1 years (range, 13.5–57 years) and time from disease onset to wheelchair use was 17.9 ± 7.0 years (range, 11–28 years). A total of 66.7% of these compound heterozygous participants (n = 8/12) reported that they were not using a wheelchair.

3.8. Questionnaire response compared to medical records

Questionnaires from 17 participants (NCNP outpatient participants) were compared to available medical records (Table 2). Age at disease onset, age at onset of gait disturbance, age at walking with assistance, and age at loss of ambulation were assessed for inter-rater reliability. Age at disease onset, age at onset of gait disturbance, age at walking with assistance, and age at loss of ambulation were assessed for inter-rater reliability. ICC values were 0.979 (95% CI 0.941–0.992) for age at disease onset, 0.917 (95% CI 0.752–0.972) for age at onset of gait disturbances, 0.985 (95% CI 0.949–0.995) for age at walking with assistance, and 0.967 (95% CI 0.855–0.993) for age at loss of ambulation.

4. Discussion

The present study provides a detailed overview of disease severity and progression in 71 Japanese participants with genetically confirmed GNE myopathy. Questionnaire-based surveys have been used to study

Please cite this article as: Mori-Yoshimura M, et al, Heterozygous UDP-GlcNAc 2-epimerase and *N*-acetylmannosamine kinase domain mutations in the *GNE*..., J Neurol Sci (2012), doi:10.1016/j.jns.2012.03.016

Table 2
Comparison of disease course among genotypes.

		Total	ED/ED	ED/LD	KD/KD
Questionnaire	*n*	71	13	28	30
	Age (years old)	43.1 ± 10.7	44.2 ± 11.2	45.3 ± 13.4	40.6 ± 13.0
	Age at onset (years old)	25.5 ± 9.2	26.3 ± 7.3[+]	29.8 ± 11.0[*]	21.2 ± 5.5[*,+]
	Age at walking with assistance	31.8 ± 10.0	34.0 ± 11.1	35.6 ± 10.9[*]	27.8 ± 6.8[*]
	Duration from onset to walking with assistance	8.4 ± 6.5	7.5 ± 7.3	9.2 ± 6.5	8.0 ± 6.6
	Wheelchair user (%)	48 (67.8)	10(76.9)	14 (50.0)[*]	24 (80.0)[*]
	Wheelchair use since (age)	37.6 ± 8.6	36.4 ± 12.0	43.0 ± 8.7[*]	31.2 ± 9.3[*]
	Number of patients with lost ambulation	35 (49.8)	6(46.2)	8 (28.6)[*]	21 (70.0)[*]
	Age at lost ambulation	33.6 ± 9.2	31.2 ± 6.0	39.7 ± 9.5	32.1 ± 9.3
	Duration from onset to loss of ambulation	12.2 ± 5.2	9.8 ± 3.5	13.8 ± 6.4	12.4 ± 5.1
NCNP outpatients	*n*	17	4	8	5
	Age (years old)	43.9 ± 14.1	53.5 ± 8.9[+]	44.3 ± 16.3	35.6 ± 9.2[+]
	Age at onset (years old)	25.8 ± 9.2	33.4 ± 9.2[+]	29.6 ± 13.5	19.6 ± 4.2[+]
	Duration from onset to walking with assistance	7.5 ± 4.2	8.9 ± 5.1	8.1 ± 4.7	5.2 ± 1.5
	Wheelchair user (%)	12 (70.6)	3 (75.0)	4 (50.0)	4 (100)
	Wheelchair use since (age)	33.3 ± 12.6	47.5 ± 17.7	35.2 ± 12.4	25.8 ± 6.3
	Number of patients with lost ambulation	9 (52.9)	3 (75.0)	3 (28.6)[*]	5 (100)[*]
	Age at lost ambulation	33.8 ± 9.3	40.0 ± 0.0	39.0 ± 16.5	31.0 ± 8.2
	Duration from onset to loss of ambulation	10.7 ± 4.2	11.2 ± 5.6	11.1 ± 7.8	6.2 ± 2.6

In the questionnaire group, age at onset and age at walking with assistance were significantly younger in KD/KD patients than in ED/KD patients. The number of wheelchair users and patients with loss of ambulation was significantly higher in the KD/KD group than in the ED/KD group. In contrast, with the exception of age at onset, there were no significant differences between ED/ED and ED/KD or KD/KD patients in these clinical parameters. The ED/ED patients were older than the others, and KD/KD patients tended to show the fastest progression.

[*] $p<0.05$ between ED/KD and KD/KD.

[+] $p<0.05$ between ED/ED and KD/KD.

the natural disease course of other rare neuromuscular disorders, such as Pompe disease [18] and spinal muscular atrophy type-1 [19]. It is difficult to establish the natural history of such rare disorders using medical records only because patients are typically seen in many different hospitals. In the present study, we used a self-reporting questionnaire and support its use for complementing medical records because it provides a more complete disease overview and establishes specific clinical trends or correlations. Indeed, our questionnaire demonstrates excellent inter-rater reliability against medical records and yields several findings regarding differences in disease progression among genetically distinct, GNE myopathy participants.

Only 15.5% of participants could walk and 7.0% could walk up stairs without assistance, which reflects the fact that GNE myopathy patients often require canes and/or leg braces at an early disease stage. This indicates that traditional six-minute walk or four-step walking tests often used to evaluate muscular dystrophies or myopathies can only be applied in a very limited number of cases, such as natural disease course studies or clinical trials. Therefore, alternate evaluation tools are required, which should include functional measurements that can be completed without canes or braces. For example, the Gross Motor Function Measure is a useful tool for evaluating mildly and severely affected patients [20].

The male to female ratio in our study population (27 males and 44 females) was skewed from the expected ratio for autosomal recessive inheritance. However, the male to female ratio of the 17 NCNP outpatient participants was 9:8. One possible explanation for the observed sex ratio in our study population is that female participants tend to be more enthusiastic toward questionnaire-based and/or PADM activities. There was no significant difference in age at survey and age at disease onset between male and female participants. However, in a mouse model of GNE myopathy, weight loss and muscle atrophy were more pronounced and occurred earlier in females compared to males [11].

We showed that KD/KD mutations are associated with a more severe phenotype compared to ED/KD mutations. Indeed, KD/KD participants had an earlier disease onset, a more rapid and progressive disease course, and a shorter time from disease onset to loss of ambulation. This was also observed in the 17 NCNP outpatient participants analyzed in our study. In contrast, ED/ED participants did not show significant differences across disease course parameters analyzed except for an earlier and later age at disease onset compared to ED/KD and KD/KD participants, respectively. Thus, ED/ED participants appear to have a disease severity intermediate between ED/KD and KD/KD participants. One possible explanation is that the major mutation, p.V572L, may be associated with a more severe phenotype. In general, the reasons for this earlier onset and disease progression remain unknown. Jewish GNE myopathy patients with homozygous p.M712T mutations have a milder phenotype compared to Japanese patients, as most of their quadriceps are spared and they usually become wheelchair-bound 15 years or more after disease onset [13,21]. Our study population included two women with homozygous p.M712T mutations: a 38 year-old ambulant and a 35 year-old non-ambulant participant. Although the two participants had a slightly later disease onset (ages 23 and 27 years, respectively) compared to KD/KD participants, the difference was not significant.

An asymptomatic patient with a p.D176V homozygous mutation was previously reported [3]. The study suggested that p.D176V homozygous patients may show a mild or late disease onset phenotype. The results presented here may support this observation as no p.D176V homozygous participants were present in our study

Table 3
Inter-rater reliability of the questionnaire.

	Onset	Age of gait disturbance	Age of gait with help	Age at loss of ambulant
Number of patients	17	17	13	9
ICC (95% CI)	0.979 (0.941–0.992)	0.917 (0.752–0.972)	0.985 (0.949–0.995)	0.967 (0.855–0.993)
p	0.000	0.000	0.000	0.000

Age at onset, age at onset of gait disturbances, age at walking with assistance, and age at loss of ambulation were assessed in a subgroup of 17 outpatients to evaluate the inter-rater reliability of the questionnaire.

Please cite this article as: Mori-Yoshimura M, et al. Heterozygous UDP-GlcNAc 2-epimerase and *N*-acetylmannosamine kinase domain mutations in the *GNE*... J Neurol Sci (2012), doi:10.1016/j.jns.2012.03.016

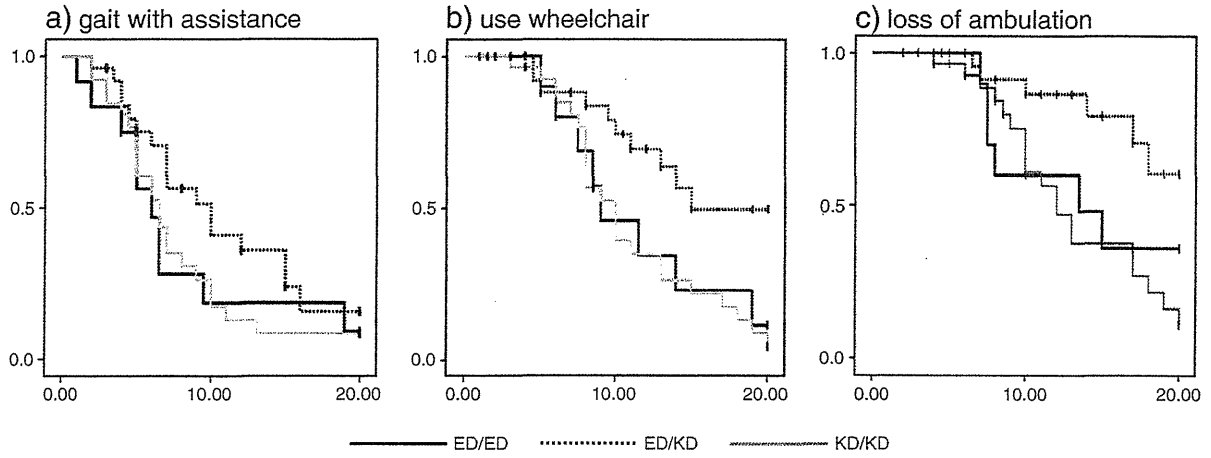

Fig. 1. Kaplan–Meier analysis of time from disease onset to (a) walking with assistance, (b) wheelchair use, and (c) loss of ambulation. Significant differences between ED/KD and KD/KD genotypes were identified. Age at disease onset was significantly different between ED/ED participants and ED/KD and KD/KD participants.

population, although p.D176V was the second most common mutation carried by 29 of our participants. In addition, a high variability was observed regarding age at disease onset and disease progression, underscoring the role of a yet-to-be identified factor(s) in determining disease phenotype.

The recruitment of participants from PADM and highly specialized neurology hospitals is a potential source of selection bias and thus a limitation of this study. These participants are likely to be more motivated because they are more severely affected compared to the general patient population. Furthermore, patients with lower disease severity may not yet be diagnosed with GNE myopathy. Therefore, our study may not accurately reflect the general patient population. Nevertheless, we believe our findings provide important information as our study population covers a broad range in age (22 to 81 years) and symptoms (minimal to wheelchair-bound). Finally, recall bias may also affect results presented in this retrospective study. Therefore, future studies should be performed with an emphasized prospective design.

In conclusion, our study shows that the KD/KD genotype (*i.e.*, p.V572L homozygous mutation) is associated with a more severe phenotype compared to compound heterozygous ED/KD mutations. Because only a small number of participants could walk, future studies should include ambulation-independent motor tests to yield a more comprehensive clinical overview in GNE myopathy patients with different genotypes.

Supplementary data to this article can be found online at doi:10.1016/j.jns.2012.03.016.

Conflict of interest

We certify that there is no conflict of interest with any financial organization regarding the material discussed in the manuscript.

Acknowledgments

We thank members of the Patients Association for Distal Myopathies (PADM) for their help. This work was partly supported by the Research on Intractable Diseases of Health and Labor Sciences Research Grants; Comprehensive Research on Disability Health and Welfare Grants, Health and Labor Science Research Grants; Intramural Research Grant (23-4, 23-5) for Neurological and Psychiatric Disorders of NCNP; and a Young Investigator Fellowship from the Translational Medical Center, NCNP.

References

[1] Nonaka I, Sunohara N, Satoyoshi E, Terasawa K, Yonemoto K. Autosomal recessive distal muscular dystrophy: a comparative study with distal myopathy with rimmed vacuole formation. Ann Neurol 1985;17:51–9.
[2] Argov Z, Yarom R. "Rimmed vacuole myopathy" sparing the quadriceps. A unique disorder in Iranian Jews. J Neurol Sci 1984;64:33–43.
[3] Nishino I, Noguchi S, Murayama K, Driss A, Sugie K, Oya Y, et al. Distal myopathy with rimmed vacuoles is allelic to hereditary inclusion body myopathy. Neurology 2002;59:1689–93.
[4] Eisenberg I, Avidan N, Potikha T, Hochner H, Chen M, Olender T, et al. The UDP-N-acetylglucosamine 2-epimerase/N-acetylmannosamine kinase gene is mutated in recessive hereditary inclusion body myopathy. Nat Genet 2001;29:83–7.
[5] Kayashima T, Matsuo H, Satoh A, Ohta T, Yoshiura K, Matsumoto N, et al. Nonaka myopathy is caused by mutations in the UDP-N-acetylglucosamine-2-epimerase/N-acetylmannosamine kinase gene (GNE). J Hum Genet 2002;47:77–9.
[6] Keppler OT, Hinderlich S, Langner J, Schwartz-Albiez R, Reutter W, Pawlita M. UDP-GlcNAc 2-epimerase: a regulator of cell surface sialylation. Science 1999;284:1372–6.
[7] Malicdan MC, Noguchi S, Nishino I. Recent advances in distal myopathy with rimmed vacuoles (DMRV) or hIBM: treatment perspectives. Curr Opin Neurol 2008;21:596–600.
[8] Noguchi S, Keira Y, Murayama K, Ogawa M, Fujita M, Kawahara G, et al. Reduction of UDP-N-acetylglucosamine 2-epimerase/N-acetylmannosamine kinase activity and sialylation in distal myopathy with rimmed vacuoles. J Biol Chem 2004;279:11402–7.
[9] Broccolini A, Gidaro T, De Cristofaro R, Morosetti R, Gliubizzi C, Ricci E, et al. Hyposialylation of neprilysin possibly affects its expression and enzymatic activity in hereditary inclusion—body myopathy muscle. J Neurochem 2008;105:971–81.
[10] Salama I, Hinderlich S, Shlomai Z, Eisenberg I, Krause S, Yarema K, et al. No overall hyposialylation in hereditary inclusion body myopathy myoblasts carrying the homozygous M712T GNE mutation. Biochem Biophys Res Commun 2005;328:221–6.
[11] Malicdan MC, Noguchi S, Nonaka I, Hayashi YK, Nishino I. A Gne knockout mouse expressing human GNE D176V mutation develops features similar to distal myopathy with rimmed vacuoles or hereditary inclusion body myopathy. Hum Mol Genet 2007;16:2669–82.
[12] Malicdan MC, Noguchi S, Hayashi YK, Nonaka I, Nishino I. Prophylactic treatment with sialic acid metabolites precludes the development of the myopathic phenotype in the GNE myopathy mouse model. Nat Med 2009;15:690–5.
[13] Argov Z, Eisenberg I, Grabov-Nardini G, Sadeh M, Wirguin I, Soffer D, et al. Hereditary inclusion body myopathy: the Middle Eastern genetic cluster. Neurology 2003;60:1519–23.
[14] Tomimitsu H, Shimizu J, Ishikawa K, Ohkoshi N, Kanazawa I, Mizusawa H. Distal myopathy with rimmed vacuoles (DMRV): new GNE mutations and splice variant. Neurology 2004;11:1607–10.
[15] Yabe I, Higashi T, Kikuchi S, Sasaki H, Fukazawa T, Yoshida K, et al. GNE mutations causing distal myopathy with rimmed vacuoles with inflammation. Neurology 2003;12:384–6.
[16] Chu CC, Kuo HC, Yeh TH, Ro LS, Chen SR, Huang CC. Heterozygous mutations affecting the epimerase domain of the GNE gene causing distal myopathy with rimmed vacuoles in a Taiwanese family. Clin Neurol Neurosurg 2007;109:250–6.
[17] Ro LS, Lee-Chen GJ, Wu YR, Lee M, Hsu PY, Chen CM. Phenotypic variability in a Chinese family with rimmed vacuolar distal myopathy. J Neurol Neurosurg Psychiatry 2005;76:752–5.

Please cite this article as: Mori-Yoshimura M, et al. Heterozygous UDP-GlcNAc 2-epimerase and *N*-acetylmannosamine kinase domain mutations in the *GNE*..., J Neurol Sci (2012), doi:10.1016/j.jns.2012.03.016

[18] Hagemans ML, Winkel LP, Van Doorn PA, Loonen MC, Hop WJ, Reuser AJ, et al. Clinical manifestation and natural course of late-onset Pompe's disease in 54 Dutch patients. Brain 2005;128:671–7.
[19] Oskoui M, Levy G, Garland CJ, Gray JM, O'Hagen J, De Vivo DC, et al. The changing natural history of spinal muscular atrophy type 1. Neurology 2007;69: 1931–6.
[20] Sienko Thomas S, Buckon CE, Nicorici A, Bagley A, McDonald CM, Sussman MD. Classification of the gait patterns of boys with Duchenne muscular dystrophy and their relationship to function. J Child Neurol 2010;25:1103–9.
[21] Eisenberg I, Grabov-Nardini G, Hochner H, Korner M, Sadeh M, Bertorini T, et al. Mutations spectrum of GNE in hereditary inclusion body myopathy sparing the quadriceps. Hum Mutat 2003;21:99.

Please cite this article as: Mori-Yoshimura M, et al. Heterozygous UDP-GlcNAc 2-epimerase and *N*-acetylmannosamine kinase domain mutations in the *GNE*..., J Neurol Sci (2012), doi:10.1016/j.jns.2012.03.016

Simple Magnetic Swallowing Detection System

Akihiko Kandori, Toshiyuki Yamamoto, Yuko Sano, Mitsuru Oonuma, Tsuyoshi Miyashita, Miho Murata, and Saburo Sakoda

Abstract—**A magnetic swallowing-detection system that can detect swallowing sounds and measure the distance between two magnetic coils was developed to detect the swallowing function non-invasively. The coils were set on both sides of the thyroid cartilage, and the distance between them changes in accordance with the movement of the thyroid cartilage. Swallowing sounds were detected by a piezoelectric microphone attached to the neck. The coils and microphone were installed in a holding unit that can be positioned at the front of the neck. The system was simultaneously used with videofluorography (VF) to measure nine healthy subjects while they swallowed liquid barium. To evaluate the correlation between the swallowing event detected by the magnetic swallowing-detection system and the swallowing event obtained from VF, two-dimensional positions of the hyoid bone in each VF image were detected. Based on the detection results, the swallowing starting time that was detected by the magnetic swallowing-detection system coincided with that determined from VF, namely, 38±172 ms. The coincidence among the peak time point of VF, that of the distance between the magnetic coils, and that of the swallowing sound appeared to have an intraclass correlation coefficient of 0.9. Correlation between the peak time points of the VF tracking waveforms, the peak time points of distance between the magnetic coils, and the peak timing of the swallowing sound had an intraclass correlation coefficient of 0.9. It can be concluded that the magnetic swallowing-detection system can detect swallowing movements simply and non-invasively without x-ray exposure.**

Index Terms—**Magnetic field, pharynx, swallowing, swallowing sound.**

I. Introduction

THE act of swallowing can be divided into four physiological phases: oral preparatory, oral, pharyngeal, and esophageal [1], [2]. In the oral stage, the tongue plays an important role in processing the food to be swallowed and in transporting the processed food from the oropharynx to the hypopharynx [3]. In the pharyngeal phase, the palatopharyngeus muscle and the stylopharyngeus muscle raise and shorten the pharynx, and the three constrictor muscles (superior, middle, and inferior) contract the pharynx [1]. Ever since videofluorography (VF) investigation of the four-stage mechanism of swallowing was introduced, [4]–[6] VF has been used to study the swallowing mechanism by analyzing, for example, the displacement of the hyoid bone [7], [8] and the size of the bolus [8], [10].

During normal swallowing, the hyoid bone moves along a triangular path: upward, forward, and back to the starting position [2], [11]. It has been reported that the upward displacement in the triangular movement is related primarily to events in the oral cavity, while the forward displacement is related to the pharyngeal processes [7]. Furthermore, a significant difference in the forward displacement of the hyoid bone was found between younger and older subjects [8]. Although the VF patterns have been analyzed to understand the swallowing mechanism, the actual mechanism is still debated due to various complexities that affect it, depending on the type and volume of the bolus [1].

The application of VF recording is limited to patients with abnormalities in swallowing function because it involves x-ray exposure. Several methods to investigate the swallowing function have therefore been developed. Some examples are the use of a non-invasive tool such as a pressure sensor for detecting tongue movement [12], a piezo-electric pulse transducer and EMG electrodes for detecting skin movement [13], impedance pharyngography for detecting electric-impedance changes [14], and a photo-reflective sensor, EMG, and tools to detect swallowing sounds for detecting laryngeal motion [15]. Although these tools provide new information on the swallowing function or dysphasia, they are not as effective as VF for evaluating the swallowing function due to the difficulty in adequately positioning or attaching the electrode.

In this study, a new magnetic electrode-less swallowing-detection system which estimates the length between magnetic coils [16]–[18] and detects swallowing sounds, was developed in order to monitor the swallowing function.

II. Methods

A. Subjects

The swallowing movement of nine normal control subjects (five males; four females; average age: 37±9 years old; age range: 26 to 48 years old) was measured using a magnetic swallowing-detection system and videofluorography (VF) (see Section III). Subjects without a history of neurological problems were defined as the normal controls. Informed consent was obtained from all subjects participating in the evaluation, which was approved by the ethical committee of the National Center Hospital of Neurology and Psychiatry.

Manuscript received July 30, 2011; revised August 21, 2011; accepted August 24, 2011. Date of publication September 08, 2011; date of current version February 08, 2012. The associate editor coordinating the review of this manuscript and approving it for publication was Dr. Subhas Mukhopadhyay.

A. Kandori, Y. Sano, and T. Miyashita are with the Central Research Laboratory, Hitachi, Ltd., Tokyo, 185-8601, Japan (e-mail: akihiko.kandori.vc@hitachi.com, yuko.sano.hd@hitachi.com, tsuyoshi.miyashita.wu@hitachi.com).

T. Yamamoto and M. Murata are with the National Center of Neurology and Psychiatry, Department of Neurology, Tokyo, 187-8551, Japan (e-mail: yamamoto@ncnp.go.jp, mihom@ncnp.go.jp).

M. Oonuma is with the Design Division, Hitachi, Ltd., Tokyo, 107-6323, Japan (e-mail: mitsuru.onuma.ej@hitachi.com).

S. Sakoda is with the Toneyama National Hospital, Osaka 560-8552, Japan (e-mail: sakoda@toneyama.go.jp).

Digital Object Identifier 10.1109/JSEN.2011.2166954

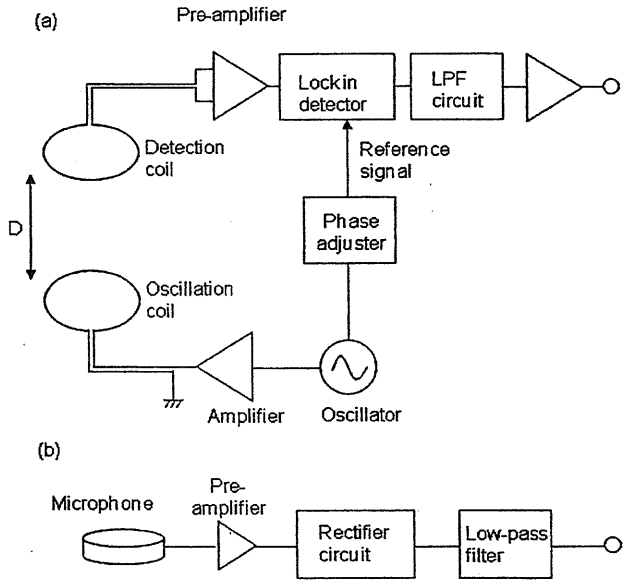

Fig. 1. Block diagram of the magnetic swallowing-detection system. (a) Distance D between two coils is estimated from magnetic-field magnitude. A magnetic field with 20-kHz frequency is generated by the oscillator, and the induced magnetic field is detected by a detection coil and demodulated by a lock-in amplifier. (b) The swallowing sound is detected by a piezoelectric microphone, and the output signal of the detected sound is rectified. The rectified sound passes through a low-pass filter.

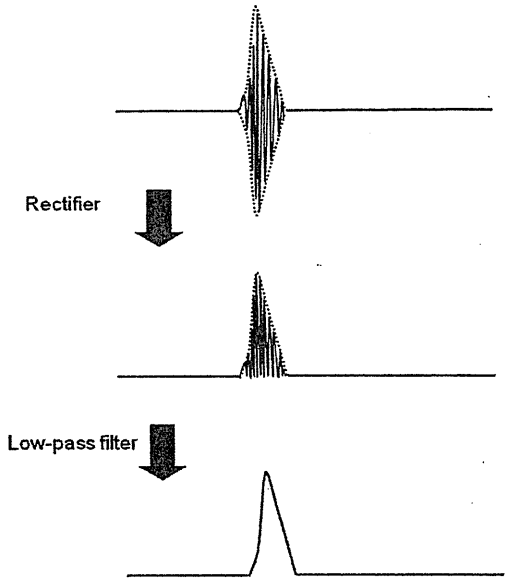

Fig. 2. Block diagram of rectified and low-pass-filtered sound.

B. Magnetic Swallowing-Detection System

The movement of the thyroid cartilage was measured by two coils, whose positions varied according to the rise and fall or the back-and-forth movements of the thyroid cartilage (or both). The swallowing sounds were detected by a piezoelectric microphone placed on the neck of the subject near the coils (Fig. 3).

A coil-length measurement system (Fig. 1(a)) detected the length (D) between the two coils (detection and oscillation), which were set on both ends of the thyroid cartilage (Fig. 1(a)). The principle of the measurement system is explained as follows. The oscillation coil produces a magnetic field with a frequency of 20 kHz, and the inductive voltage in the detection coil is detected in the same manner as a conventional finger-tapping measurement system [16]–[18]. The voltage is demodulated and passed through a low-pass filter (cutoff frequency < 30 Hz). The voltage is converted to D using calibration data measured by the relationship between D and the voltage.

The piezoelectric microphone in the swallowing-sound detection system (Fig. 1(b)) was used to detect only contacting sound without interference noise. The sound voltage detected by the microphone was rectified and passed through a low-pass filter to detect its envelope (as shown in Fig. 2). Detecting the envelope of the sound wave in this manner made it possible to acquire the swallowing sound data using a low sampling frequency (i.e., 100 Hz).

The swallowing-detection system is simply composed of three parts: a holder unit (containing the built-in coils and microphone), a detection-circuit unit, and a personal computer for controlling and recording the detected-sound signal and the measured coil-length voltage (Fig. 3(a)). The holder unit (Fig. 3(b)) is positioned at the front of the neck (Fig. 3(c)). It has two parts: one that maintains the holder shape, and another that holds the two coils against the subject's throat and follows the movement of the thyroid cartilage. This two-part structure makes it possible to attach the holder unit to subjects with different neck sizes.

The coil-length voltage and the swallowing-sound signals are converted from analog to digital format at a sampling rate of 100 Hz. The start time and length of the analog-to-digital sampling are controlled by the PC.

C. Simultaneous Measurements by Videofluorography and Magnetic Swallowing-Detection System

Videofluorography (Sonialvision Plus, Shimazdu Ltd.) was used to measure the swallowing movement of subjects positioned in the lateral position. VF images were recorded by a digital video recorder onto a DVD at 30 frames per second. The subjects drank diluted barium sulfates (10 ml) with water, which were injected into the mouth by a syringe on cue at the start of the VF measurement. Before starting the VF measurement, each subject fitted the holder unit of the magnetic swallowing-detection system themselves, and the holder unit was checked to verify that it did not hinder the recording of VF images.

The holder unit was tapped with a small metal bar, and the tapping sound was detected by the microphone in the magnetic swallowing-detection system. The movement of the metal bar was simultaneously recorded as a shadow in a VF image. These tapping recording data were used to adjust the start timing of the measurements by both the magnetic swallowing-detection system and VF. The tap timings recorded by both systems were detected, and the two measured times were compared.

D. Data Analysis

Two-dimensional positions of the hyoid bone in each VF image were detected, and the movement waveforms (back-and-forth direction (x-axis)) and the rise-and-fall direction (y-axis)) of the hyoid bone were produced by using tracking

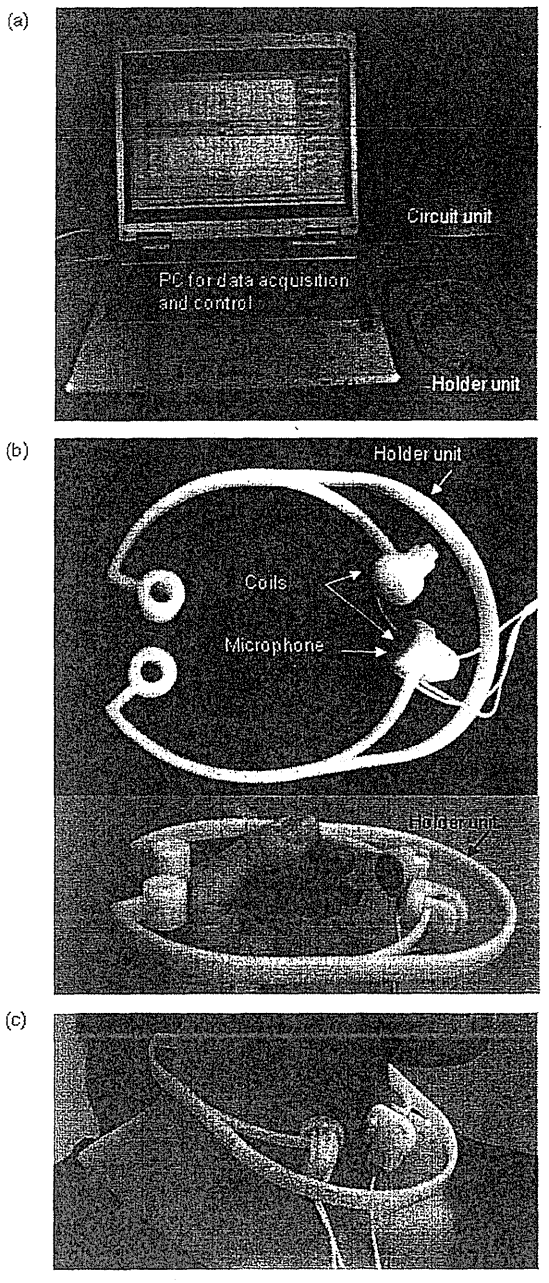

Fig. 3. (a) Photograph of the magnetic swallowing-detection system. The PC controls the circuit unit and collects the detection data. (b) Holder unit: the two coil parts (one contains the microphone) in the holder unit are pressed against the neck to establish good contact. To attain good sound transmission, the microphone is set in the top position in one coil part. (c) Holder unit attached to the neck of a subject.

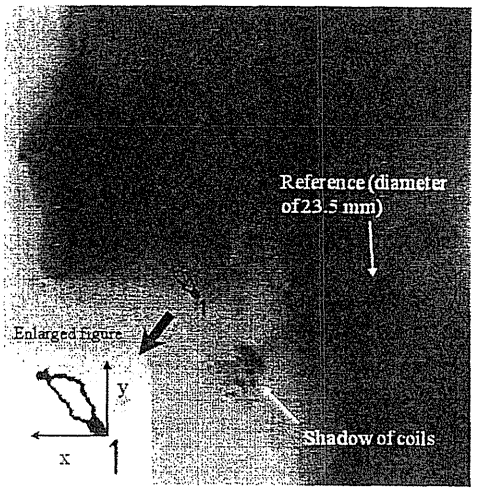

Fig. 4. Sample VF image. A copper coil (with a diameter of 25.5 mm) is positioned at the side of the neck as a reference. The coil shadow, along with the hyoid bone and the bolus, can be clearly seen. From the VF images, the tracking line of the hyoid bone can be detected during swallowing.

software ("Move Tr 2D") (Fig. 4). The hyoid-bone-tracking waveforms were resampled at a sampling interval of 10 ms after spline interpolation to adjust the sampling time of the magnetic swallowing-detection system. To determine the position of diluted barium sulfates as they were swallowed, the starting and ending transit times of four fields (oral cavity (OC), upper oropharynx (UOP), valleculae (VAL), and hypopharynx (HYP); see Fig. 6, lower figure, by Saitoh *et al.* [19]) during the swallowing were determined from the VF images. On the other hand, the sound and coil-distance waveforms measured by the magnetic swallowing-detection system were not preprocessed because the sampling rate of the VF waveforms was adjusted to that of the magnetic swallowing-detection system (Fig. 5, upper graph).

After the VF waveforms were preprocessed, the characteristic times (P1, N2, P3, N4, P5, S1, Smax, S2, VF1, VF2, VF3, and VF4, in Fig. 5) in each VF waveform and in each magnetic swallowing-detection waveform were determined visually. To make it easier to understand the typical swallowing-detection waveforms, the amplitude of coil distance and the sound waveforms at times P1, N2, P3, N4, and P5 were also measured. Statistical differences between these times were tested by using the intraclass correlation coefficient (ICC).

III. Results

A. Typical VF and Magnetic Swallowing-Detection System Waveforms

The coil-distance waveform had a "W" shape, and the sound waveform had several peaks (Fig. 5). Five characteristic times (start time P1, three peaks in the W-waveform (N2, P3, and N4), and end time P5) could therefore be detected. Because several peaks appeared in the sound waveforms of each subject, only three times (start time S1, peak time Smax, and end time S3) were detected. In the VF waveform, an "x component" of the VF waveform indicated that the hyoid bone moved in a fourth direction and returned to its original position. A "y component" of the VF waveform indicated that the hyoid bone moved in the upper direction and returned to its original position. As for the characteristic times in these VF waveforms, only one time point (peak time VF1) was detected in the x-component, and only two time points (start time VF2 and end time VF3) were detected in the y-component because each subject had a variety of y-component waveforms. The absolute variance of the VF waveforms was calculated from the square root of the x- and

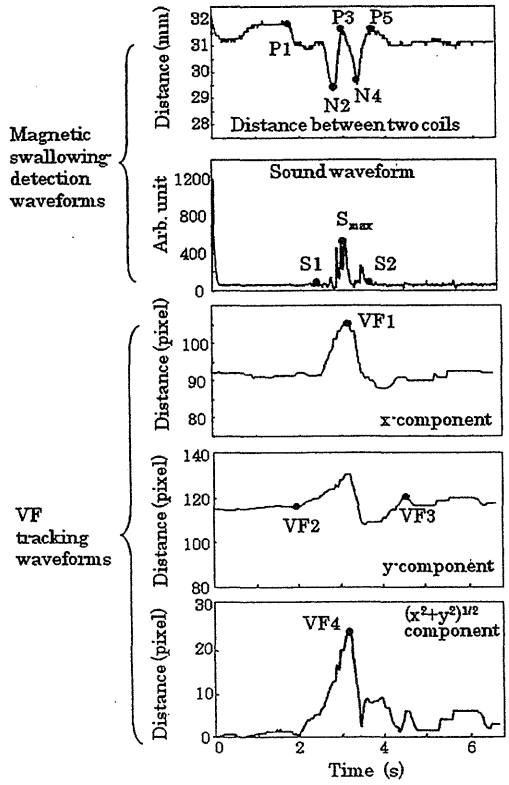

Fig. 5. Typical waveforms recorded by magnetic-swallowing detection and VF tracking. In the distance waveform (top one), five time points (P1, N2, P3, N4, and P5) are detected. Three time points are detected in the corresponding sound waveform. In the VF tracking waveform, a peak VF1 of the x-component, beginning at VF2 and ending at VF3 of the y-component are detected. In the absolute waveform recorded by the VF tracking, the peak time VF4 is detected.

y-components of the VF waveform, so the peak time (VF4 in the bottom waveform in Fig. 5) could therefore be detected.

B. Time Variance of Swallowing

N2 and S1 at the primary negative peak (PNP) appear at the end of OC and the beginning of UOP and VAL (Fig. 6(a) and (b)). P3, Smax, VF1, and VF4 at the PP appear in the middle of HYP.

Although the ICC for P1 and VF2 in SP could not be calculated because P1 was defined as a standard time (0 s), the average VF2 was 38 ms (Fig. 6(a) and Table I). The four peak times P3, Smax, VF1, and VF4, which indicated the peak HYP time, were high, i.e., ICC > 0.9 (Table I). The ICC for N2 and S1 in PNP was 0.54, and that between N4 and S2 in SNP was 0.68. However, the ICC for P5 and VF3 in EP was 0.1.

C. Mean Coil Distance and Sound Waveforms

The mean coil distance appeared as a W-shaped waveform, and the mean sound waveform showed a one-peak waveform (Fig. 7). The W-shaped waveform means that the coil distance was shortened at N2, widened to the original distance at P3, shortened again at N4, and finally widened to the original distance. This shortening and widening produced the W shape in the detected magnetic-swallowing waveform. Although the swallowing sound appeared within the duration from N2 to N4

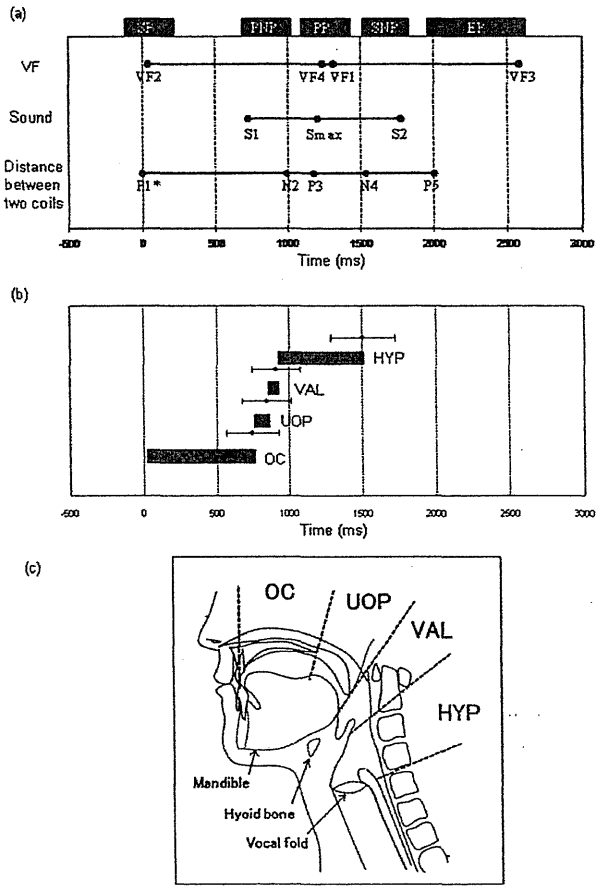

Fig. 6. (a) Characterized average time and standard deviation obtained from each waveform of nine normal controls. (b) Start and end times of swallowing 10 cc of liquid barium in the four fields (OC, UOP, VAL and HYP). The four-field time durations are also indicated as gray bars. (c) Four defined fields.

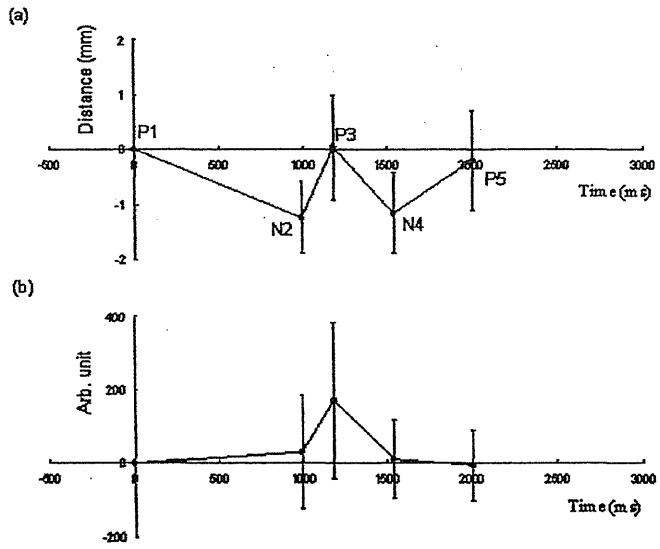

Fig. 7. (a) Mean coil distance at times (P1), (N2), (P3), (N4), and (P5) plotted with standard deviation (see Table 1). Waveform shape is W-type. (b) Swallowing sound at times (P1), (N2), (P3), (N4), and (P5) plotted with standard deviation (see Table 1). The sound waveform has one peak.

in the coil-distance timing, an individual variation with many peaks occurs in the waveform. Consequently, with the normal

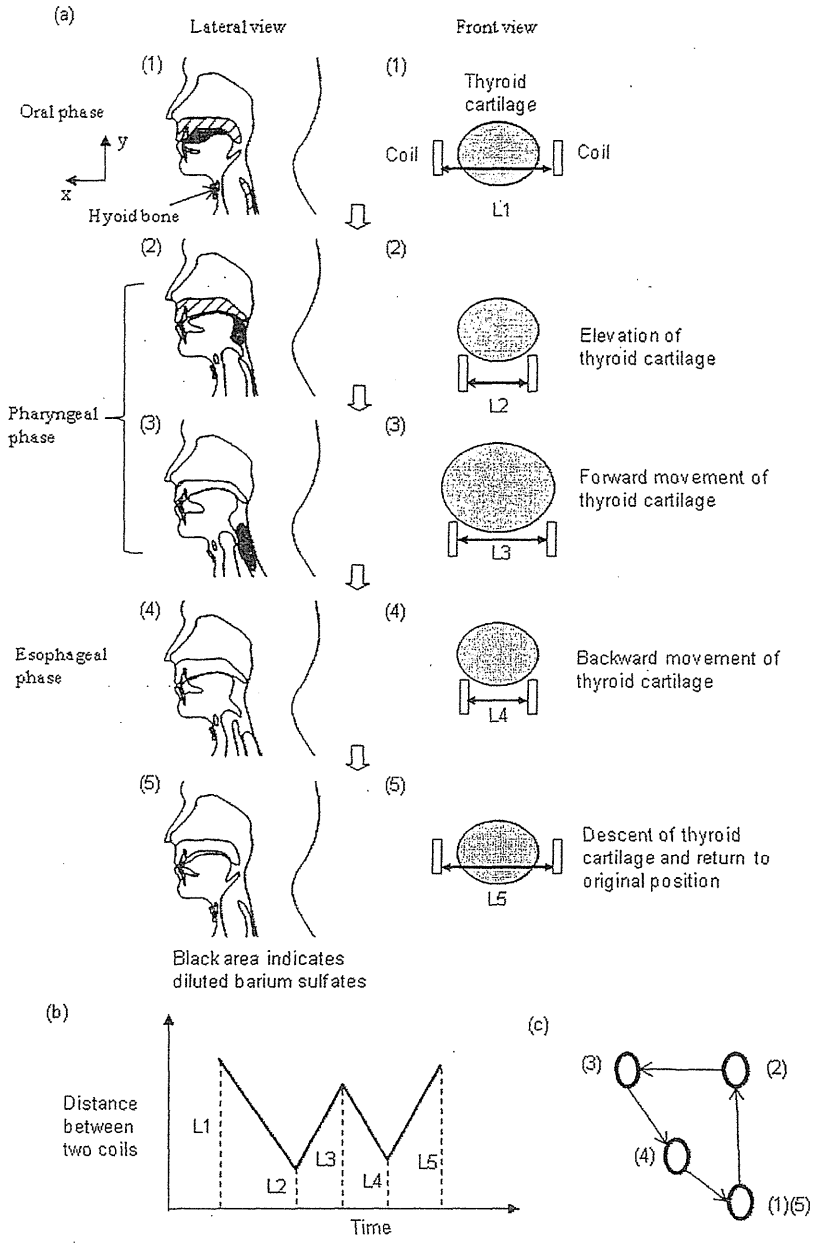

Fig. 8. (a) Relationship between liquid-barium position, coil distances (L1, L2, L3, L4, and L5), and thyroid cartilage site. (b) W-shaped waveform (Fig. 7(a)) reconstructed by using coil distance (L1, L2, L3, L4, and L5 of (a)). (c) Hyoid bone movement corresponding to (1) to (5) shown in (a).

controls, the coil distance showed a W-shaped waveform, and the swallowing sound had a one-peak waveform.

IV. Discussion

The relationship between the swallowing movement and magnetic swallowing-detection waveforms is explained as follows (see Fig. 8(a) and (b)). Coil distance L1 in the first oral phase hardly changes because the thyroid-cartilage movement changes very little. In the next pharyngeal phase, the deglutition reflex starts, and rapid laryngeal elevation occurs. The thyroid cartilage therefore goes between the two coils, and the coil distance is shortened to L2. The forward movement of the thyroid cartilage causes the coil distance to increase to L3. In the esophageal phase, the thyroid cartilage goes backward, and the coil distance is shortened to L4. After the swallowing movement, the distance decreases again to L5 (which is almost the same as L1). Therefore, it is apparent that the coil distance W-shaped waveform reflects the movement of the thyroid cartilage in the larynx, and the timing of the larynx movement can be detected based on this waveform. The correlation between the thyroid cartilage and the coil distance movements was also distinguishable by looking at their correlated movement in the VF images. Furthermore, the changes depending on the triangle movement of the hyoid bone (see Figs. 4 and 8(c)) could be seen in the coil distance waveforms because the main timings (P1 and P3) of the coil

TABLE I
SUMMARIZED TIME-VARIANCE LIST OF SWALLOWING. THE * INDICATES THE START TIME OF SWALLOWING. ITALICIZED NUMBERS INDICATE INTRACLASS CORRELATION COEFFICIENTS. FIVE TIMES ARE DEFINED: START POINT (SP), PRIMARY NEGATIVE PEAK (PNP), POSITIVE PEAK (PP), SECONDARY NEGATIVE PEAK (SNP), AND END POINT (EP)

Waveform	VF	Sound	Coils
SP	VP2 38 ± 172 ms	–	P1* 0
PNP	–	S1 0.73 ± 0.52 s	N2 0.99 ± 0.30 s
		0.54	
PP	VF1 1.31 ± 0.45 s	Smax 1.21 ± 0.49 s	P3 1.18 ± 0.32 s
	0.91		*0.89*
	VF4 1.24 ± 0.35 s		
	0.93		
SNP	–	S2 1.77 ± 0.52 s	N4 1.53 ± 0.32 s
		0.68	
EP	VF3 2.58 ± 0.40 s	–	P5 2.00 ± 0.47 s
		0.10	

distance waveform were correlated with those (VF1, VF2, and VF4) of the VF waveforms.

When the magnetic swallowing-detection system measures the above-mentioned thyroid-cartilage movement, it might detect abnormalities in the swallowing movement as aspiration. If the time duration from N2 to P3 reflects a rapid laryngeal elevation after the deglutition reflex, the closure delay of the larynx causes the aspiration. It has been reported that the swallowing time is delayed [20] and the forward movement of the hyoid bone decreases [8] in accordance with the increasing age of the subjects. It can therefore be inferred that the long time from N2 to P3 is often seen in elderly people, and the insufficient forward movement of the thyroid cartilage (which depends on muscle weakness) produces an unclear P3 peak and monophasic wave shape (i.e., not a W-shape). Furthermore, the reduced time from N2 to N4 indicates the lack of elevation time of the larynx because it is thought that the bolus passes to the hypopharynx at time N4.

Although the mechanism that produces the swallowing sound is still not clear, the sound occurs when the bolus goes from the pharynx to the esophagus [21]. It is therefore thought that the peak Smax appears at the same time. The evaluation of the swallowing movement using both the coil length and the sound waveforms makes it possible to determine the correct deglutition reflex by using the coil-length changes when no swallowing sound occurs.

It has been reported that there is no correlation between the amplitudes of upward and forward displacements of the hyoid bone, and that the amplitude of the upward displacement is highly variable [7]. However, the magnetic swallowing-detection system obtained a W-shaped waveform of coil distance and a monophasic sound waveform, which were similar to the hyoid-bone tracking waveform determined by VF. These waveforms were invariable among healthy subjects. It can be concluded that the magnetic swallowing-detection system can detect swallowing movement more simply and non-invasively than a hyoid-movement detection system.

V. LIMITATIONS

There are several limitations to this study. One is that the magnetic swallowing-detection system cannot detect the position of the bolus or the degree of thyroid-cartilage elevation. Another is the small number of subjects used; further study with a larger sample is needed to confirm our findings. Finally, the measurement reliability of the magnetic swallowing-detection system was not evaluated. Therefore, further study for the reliability is needed. The system, however, can simply and noninvasively evaluate the swallowing movement.

ACKNOWLEDGMENT

The authors are grateful to T. Ono of Osaka University, Graduate School of Dentistry for discussing the swallowing mechanism with us. We also thank K. Morohoshi, K. Ishizuka, and N. Matsumoto of Hitachi Computer Peripherals Co., Ltd. for developing the magnetic swallowing-detection system.

REFERENCES

[1] M. A. Crary and M. E. Grother, *Butterworth Heinemann Elsevier 2003* (in Japanese), I. Fujishima, Ed. : Ishiyaku Publishers, Inc., 2007.
[2] J. A. Logemann, *Pro-ed.* Austin, TX: , 1998.
[3] T. Ono, K. Hori, Y. Masuda, and T. Hayashi, "Recent advancement in sensing oropharyngeal swallowing function in Japan," *Sensors. 10*, vol. 176, pp. 176–202, 2010.
[4] J. B. Saunders, C. Davis, and E. R. Miller, "The mechanism of deglutition (second stage) as revealed by cine-radiography," *Ann. Otol. Rhinol. Laryngol.*, vol. 60, no. 4, pp. 897–897, 1951.
[5] G. H. Ramsey, J. S. Watson, R. Gramiak, and S. A. Weinberg, "Cinefluorographic analysis of the mechanism of swallowing," *Radiology*, vol. 64, no. 4, pp. 498–498, 1955.
[6] R. I. Roberts, "A cineradiographic investigation of pharyngeal deglutition," *Br. J. Radiol.*, vol. 30, no. 357, pp. 449–449, 1957.
[7] R. Ishida, J. B. Palmer, and K. M. Hiiemae, "Hyoid motion during swallowing: Factors affecting forward and upward displacement," *Dysphagia*, vol. 17, no. 4, pp. 262–262, 2002.
[8] Y. Kim and G. H. McCullough, "Maximum hyoid displacement in normal swallowing," *Dysphagia.*, vol. 23, no. 3, pp. 274–274, 2008.
[9] K. A. Kendall, S. McKenzie, R. J. Leonard, M. I. Gonçalves, and A. Walker, "Timing of events in normal swallowing: A videofluoroscopic study," *Dysphagia.*, vol. 15, no. 2, pp. 74–74.
[10] A. R. Wintzen, U. A. Badrising, R. A. Roos, J. Vielvoye, and L. Liauw, "Influence of bolus volume on hyoid movements in normal individuals and patients with Parkinson's disease," *Can. J. Neurol. Sci.*, vol. 21, no. 1, pp. 57–57, 1994.
[11] R. L. Shelton Jr., J. F. Bosma, and B. V. Sheets, "Tongue, hyoid and larynx displacement in swallow and phonation," *J. Appl. Physiol.*, vol. 15, pp. 283–283, 1960.
[12] T. Ono, K. Hori, and T. Nokubi, "Pattern of tongue pressure on hard palate during swallowing," *Dysphagia.*, vol. 19, no. 4, pp. 259–264, 2004.
[13] A. Toyosato, K. Ueda, and S. Nomura, "Examination of swallowing evaluation method at the bedside," (in Japanese, English) *JADS*, vol. 26, pp. 42–46, 2007.
[14] Y. Yamamoto, T. Nakamura, Y. Seki, K. Utsuyama, K. Akashi, K. Jikuya, and Neck, "Electrical impedance for measurement of swallowing," (in Japanese, English) *T. IEE Jpn.*, vol. 118-A, no. 3, pp. 210–217, 1998.
[15] T. Hayashi, H. Kaneko, Y. Nakamura, T. Ishida, H. Takahashi, Y. Yamada, N. Michimi, and S. Nomura, "Relationship between Rice-Gruel properties and swallowing motion—Evaluation by simultaneous measurement of larynx movement, electromyogram and swallowing sound," (in Japanese, English) *Jpn. J. Dysphag. Rehabil.*, vol. 6, pp. 73–81, 2002.

[16] A. Kandori, M. Yokoe, S. Sakoda, K. Abe, T. Miyashita, H. Oe, H. Naritomi, K. Ogata, and K. Tsukada, "Quantitative magnetic detection of finger movements in patients with Parkinson's disease," *Neurosci Res.*, vol. 49, pp. 253–260, 2004.
[17] A. Kandori, T. Miyashita, N. Hosono, M. Yokoe, K. Ogata, K. Abe, and S. Sakoda, "Motion analysis of grip and release with fingers using simple magnetic detection system," *Rev. Sci. Instrum.*, vol. 78, pp. 034302–034302, 2007.
[18] A. Kandori, Y. Sano, T. Miyashita, Y. Okada, M. Irokawa, K. Shima, T. Tsuji, M. Yokoe, and S. Sakoda, "Estimation method of finger tapping dynamics using simple magnetic detection system," *Rev. Sci. Instrum.*, vol. 81, pp. 054303–054303, 2010.
[19] E. Saitoh, S. Shibata, K. Matsuo, M. Baba, W. Fujii, and J. B. Palmer, "Chewing and food consistency: Effects on bolus transport and swallow initiation," *Dysphagia*, vol. 22, no. 2, pp. 100–107, 2007.
[20] I. Kaneko, "A cinefluorographic study of hyoid bone movement during deglutition," *Nippon Jibiinkoka Gakkai Kaiho.*, vol. 95, no. 7, pp. 974–87, Jul. 1992.
[21] J. A. Y. Cichero and B. E. Murdoch, "The physiologic cause of swallowing sounds: Answers from heart sounds and vocal tract acoustics," *Dysphagia*, vol. 13, no. 1, pp. 39–52, 1998.

Akihiko Kandori was born in Hiroshima, Japan, on October 25, 1965. He received the B.S. and M.S. degrees in electrical engineering, and the Ph.D. degree in engineering from Sophia University, Tokyo, Japan, in 1988, 1990, and 1997, respectively, and the Ph.D. degree in medicine from Tsukuba University, Ibaraki, Japan, in 2003.

In 1990, he joined the Central Research Laboratory, Hitachi Ltd. From 1992 to 1994, he was with the Superconducting Sensor Laboratory of National Project. He has been interested in SQUID sensor and applications for many years. He is a Chief Researcher at the Central Research Laboratory, Hitachi Ltd. His current interests are in magnetic field measurement biomedical system, biomagnetic imaging, and SQUID sensor system.

Toshiyuki Yamamoto was born in Sapporo, Japan, on November 3, 1970. He received the M.D. degree from Sapporo Medical University, Sapporo, Japan, in 1996, and the Ph.D. degree from the Tokyo Medical and Dental University, Tokyo, Japan, in 2010.

He worked in the Department of Neurology, National Center Hospital of Neurology and Psychiatry (NCNP), Tokyo, Japan, from 1999 to 2004. He studied in the Department of Physical Medicine and Rehabilitation, Johns Hopkins University, from 2004 to 2005. He has been working as a Neurologist at the Department of Neurology, NCNP, since 2005. He has an interest in physiology and kinesiology of swallowing in neurodegenerative disease and psychiatric disease. He is now involved with a study using videofluorography and the simple magnetic swallowing detection system to evaluate the swallowing function in Parkinson's disease.

Yuko Sano was born in Tokyo, Japan, on July 7, 1982. She received the B.S. and M.S. degrees in mechano-infomatics from the University of Tokyo, Tokyo, in 2005 and 2007, respectively.

In 2007, she joined the Advanced Research Laboratory, Hitachi Ltd. In 2011, she joined the Central Research Laboratory, Hitachi Ltd. She has been interested in analysis of medical and biological data using multivariable analysis or machine learning techniques. Her main research topic is to quantify severity of diseases in finger tapping data.

Mitsuru Oonuma was born in Tokyo, Japan, on May 18, 1950. He graduated from Salesian Polytechnic in 1971.

He joined the Hitachi Design Research Institute in 1971, where he worked on the industrial design of home electrification apparatus, construction machinery, and medical equipment. Now, his research interests are in industrial design of the analysis equipment.

Tsuyoshi Miyashita was born in Kagoshima, Japan, on February 6, 1963. He received the B.S. degree in physics and the M.S. degree in engineering science from Kyushu University, Fukuoka, in 1987 and 1989, respectively.

In 1989, he joined the Advanced Research Laboratory, Hitachi Ltd., Tokyo, Japan. In 2011, he joined the Central Research Laboratory, Hitachi Ltd. He has been interested in analysis of bio-electric and bio-magnetic data such as EEG, MEG, ECG, MCG. His current interest is near-infrared spectroscopy system for measuring brain functions.

Miho Murata was born in Kofu, Japan. She received the M.D. degree from the University of Tsukuba, School of Medicine, Tsukuba, Japan, in 1984, and the Ph.D. degree from the Department of Neurology, University of Tsukuba, in 1992.

She worked at the University Hospital of Tsukuba and the University of Tokyo. She is currently the Director of the Department of Neurology, National Center of Neurology and Psychiatry, Japan. Her main focus is the therapy of Parkinson's disease and she found zonisamide effects on Parkinson's disease.

Saburo Sakoda was born in Hiroshima, Japan, in 1951. He received the M.D. degree in 1975 and the Ph.D. degree in 1984 from Osaka University, Faculty of Medicine, Osaka, Japan.

After postdoctoral training at the Osaka University Hospital (April 1975–May 1985), he moved to the Research Institute of Neurology, Department of Neurology, Osaka University, to begin additional postdoctoral studies and has been developing his research in neurology (December 1986–July 1994). From 2000 to 2010, he was a Professor at the Department of Neurology. He joined the National Organization Hospital, Toneyama Hospital, Osaka, Japan, as a Medical Center Director in April 2010.

Role of the External Oblique Muscle in Upper Camptocormia for Patients with Parkinson's Disease

Patients with Parkinson's disease (PD) often experience camptocormia, a postural disorder with unclear pathophysiology and unestablished treatments.[1] We clinically categorized camptocormia as upper and lower types based on the location of inflection points. We defined upper camptocormia as abnormal truncal flexion at a point between the lower thoracic and upper lumbar vertebrae whose flexion angle exceeded 40 degrees, whereas lower camptocormia was defined as abnormal truncal flexion at the hip joint. This study focused on upper camptocormia.

We performed lidocaine injections into the abdominal muscles of PD patients with upper camptocormia and evaluated their effects on posture to investigate its pathophysiology. Patients with fixed posture because of spinal disease or truncal muscle weakness were excluded. We included 5 patients (4 women and 1 man; mean age, 70.8 ± 4.4 years; PD duration, 8.2 ± 3.9 years; Hoehn & Yahr stage, 2.6 ± 0.8) treated with antiparkinson drugs in our hospital. Camptocormia did not respond to these drugs in any of the patients. Ultrasound guidance was used for lidocaine injections into the abdominal muscle (rectus abdomen [RA] and external oblique [EO] in all patients; internal oblique [IO] in 2 patients; 50 mg in each muscle bilaterally). Although the order of each injection was different in each patient, the following injection was performed on confirming that improvement diminished or if no improvement was observed after several days. Flexion angles were measured before and after each injection. The angle formed between a line perpendicular to the ground and a line linking the C7 vertebra with the inflection point of the trunk was defined as the flexion angle. This study was approved by the NCNP ethics committee. Informed consent was obtained from all patients.

The posture of all patients improved following injection into the EO. The average flexion angle decreased from 49 ± 6.0 degrees to 37 ± 10 degrees (truncal angle of age-matched PD patients without camptocormia was 29.4 ± 3.7 degrees; Fig. 1), Only 1 patient showed mild improvement after injection into the RA. No improvements were observed following injection into the IO.

The RA performs truncal anteflexion, whereas the EO and IO work bilaterally for truncal flexion. Azher et al previously reported improvement of camptocormia by botulinum toxin injection into the RA,[2] although they did not classify camptocormia by type. In the present study, forward flexion was reduced in all patients after injection into the EO, not RA nor IO. Our results may suggest that the EO is primarily associated with upper camptocormia pathogenesis. Considering that previous studies have speculated that lidocaine could suppress dystonic excitation,[3–5] dystonia of the EO may be a cause of upper camptocormia.

Although this study has some limitations, such as the small number of patients and not adjusting lidocaine dose for muscle size, this is the first report to investigate camptocormia pathophysiology by classification, and these findings may contribute to the treatment of upper camptocormia in patients with PD. To confirm our results, we have been carrying out a larger study.

Acknowledgment: We express our deepest gratitude to Dr. Atsuo Nakagawa, whose extensive support and insightful comments were invaluable during the course of our study.

Yoshihiko Furusawa, MD[1]*, Yohei Mukai, MD[1], Yoko Kobayashi, PhD[2], Takashi Sakamoto, MD[1], Miho Murata, PhD[1]

[1]Department of Neurology, National Center Hospital of Neurology and Psychiatry Kodaira, Tokyo, Japan; [2]Department of Rehabilitation, National Center Hospital of Neurology and Psychiatry Kodaira, Tokyo, Japan

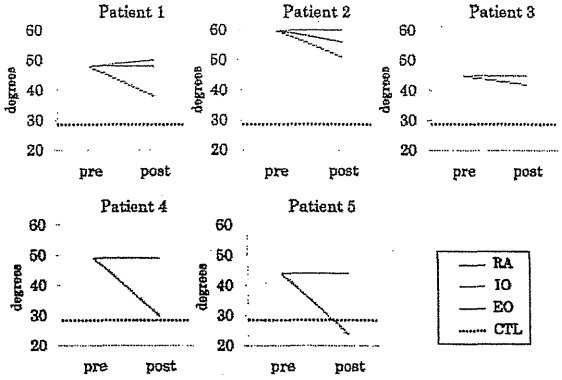

FIG. 1. Effect of lidocaine injection on camptocormia. The greatest improvement was observed after injection into the EO. The dotted line indicates the average truncal angle of control patients (RA, rectus abdomen; IO, internal oblique; EO, external oblique; CTL, control patients).

* **Correspondence to:** Yoshihiko Furusawa, Department of Neurology, National Center Hospital of Neurology and Psychiatry Kodaira, Tokyo, Japan; yfuru@ncnp.go.jp

Funding agencies: This work was supported in part by Grants-in-Aid from the Research Committee of CNS Degenerative Disease, the Ministry of Health, Labour and Welfare of Japan, and Intramural Research Grant (21B-4) for Neurological and Psychiatric Disorders of NCNP.

Relevant conflicts of interest/financial disclosures: Nothing to report. Full financial disclosures and author roles may be found in the online version of this article.

Published online in Wiley Online Library (wileyonlinelibrary.com). DOI: 10.1002/mds.24930

References

1. Melamed E, Djaldetti R. Camptocormia in Parkinson's disease. J Neurol 2006;253:VII14–VII16.
2. Azher SN, Jankovic J. Camptocormia: pathogenesis, classification, and response to therapy. Neurology 2005;65:355–359.
3. Kaji R, Rothwell JC, Katayama M, et al. Tonic vibration reflex and muscle afferent block in writer's cramp. Ann Neurol 1995;38:155–162.
4. Irwin D, Revuelta G, Lippa CF. Clinical improvement of secondary focal limb dystonia in neurodegenerative disease following a five-day lidocaine infusion: a case report. J Neurol Sci 2009;277:164–166.
5. Yoshida K, Kaji R, Kubori T, Kohara N, Iizuka T, Kimura J. Muscle afferent block for the treatment of oromandibular dystonia. Mov Disord 1998;13:699–705.

Qual Life Res (2012) 21:1299–1303
DOI 10.1007/s11136-011-0041-2

BRIEF COMMUNICATION

Validation of the Japanese translation of the Swallowing Disturbance Questionnaire in Parkinson's disease patients

Toshiyuki Yamamoto · Kensuke Ikeda · Harumi Usui · Masako Miyamoto · Miho Murata

Accepted: 5 October 2011 / Published online: 16 October 2011

Abstract
Purpose The Swallowing Disturbance Questionnaire (SDQ) was developed as a self-rated screening tool for dysphagia in patients with Parkinson's disease (PD). We developed the Japanese version of this questionnaire (SDQ-J), according to the cross-cultural adaptation guidelines, and examined its reliability.
Methods Subjects were 61 Japanese patients with PD (mean age, 67.0 ± 9.2 years) who answered the SDQ-J before undergoing videofluoroscopic examination of swallowing (VF). We compared the findings of the questionnaire with the patients' aspiration status during VF.
Results Cronbach's alpha coefficient for the 15 questions of the SDQ-J was 0.84. According to the SDQ-J, 15 patients (24.6%) were diagnosed with dysphagia, while 9 patients (14.8%) aspirated liquid during VF. The sensitivity and specificity of the SDQ-J in predicting aspiration were 77.8 and 84.6%, respectively; therefore, the SDQ-J significantly predicted aspiration during VF ($P < 0.01$). The positive predictive value (PPV) and negative predictive value (NPV) for the SDQ-J were 0.46 and 0.96, respectively.
Conclusions The SDQ-J appears to be a reliable and useful screening tool for Japanese PD patients with aspiration. As the NPV was higher than the PPV in the SDQ-J, this questionnaire could potentially be used for early identification of severe dysphagia in patients with PD.

Keywords Parkinson's disease · Dysphagia · Questionnaires · Fluoroscopy

Abbreviations

PD	Parkinson's disease
VF	Videofluoroscopic examination of swallowing
SDQ	Swallowing Disturbance Questionnaire
SDQ-J	Japanese version of the SDQ
H&Y	Hoehn–Yahr
PPV	Positive predictive value
NPV	Negative predictive value
SLP	Speech and language pathologist
FEES	Fiberoptic endoscopic evaluation of swallowing

T. Yamamoto (✉) · K. Ikeda · M. Murata
Department of Neurology, National Center Hospital of Neurology and Psychiatry, 4-1-1 Ogawahigashi-cho, Kodaira, Tokyo 187-8551, Japan
e-mail: yamamoto@ncnp.go.jp

H. Usui
Department of Nursing, National Center Hospital of Neurology and Psychiatry, 4-1-1 Ogawahigashi-cho, Kodaira, Tokyo 187-8551, Japan

M. Miyamoto
Department of Rehabilitation Medicine, National Center Hospital of Neurology and Psychiatry, 4-1-1 Ogawahigashi-cho, Kodaira, Tokyo 187-8551, Japan

Introduction

Patients with Parkinson's disease (PD) who experienced dysphagia have reported greatly reduced quality of life (QOL) [1]; therefore, early diagnosis and treatment of the dysphagia of such patients is important. Videofluoroscopic examination of swallowing (VF) is the standard method used to diagnose dysphagia; however, it cannot be frequently used because it involves exposure to X-rays. The Swallowing Disturbance Questionnaire (SDQ), a self-rated

scale comprising 15 questions regarding the frequency of the dysphagia symptoms of during every meal, was developed as a screening tool for dysphagia in PD patients ("Appendix"). The worst total score of SDQ has been 44.5 points, and dysphagia is diagnosed when the total score is 11 points or more [2]. The SDQ is not yet recommended for widespread use because it has only been tested on a relatively small number of patients in a single PD population. Its translation into other languages followed by further extensive testing of the questionnaire has, therefore, been advised [3]. Accordingly, we created a Japanese version of the SDQ (SDQ-J) and examined its reliability in relation to the patients' aspiration status during VF.

Patients and methods

Patients

The subjects of this study were 61 Japanese patients with PD who were able to consume food orally (mean age, 67.0 ± 9.2 years; 40 men, 21 women). These subjects were selected for inclusion in the study, irrespective of the subjective symptoms of dysphagia, from among 82 PD patients who were admitted for short periods to our hospital for evaluation or treatment of parkinsonism between April 6, 2010, and March 29, 2011.

All patients had been diagnosed with clinically definite PD [4] and were effectively treated with L-dopa. Cranial magnetic resonance imaging was performed on all subjects to exclude cerebral infarction and other neurodegenerative disorders. We excluded patients with other diseases that cause dysphagia and those who were being fed by tube or undergoing treatment for complications such as dehydration, pneumonia, delirium, or depression. Patients who had undergone VF within the previous year were also excluded to avoid overexposure to excessive radiation. Patients who could not fill out the questionnaire by themselves because of parkinsonism or dementia were also excluded.

This study was approved by the ethics committee of our institution (A2010-003), and written informed consent was obtained from all patients before beginning this study.

Japanese version of the Swallowing Disturbance Questionnaire

We created the SDQ-J according to the guidelines for the cross-cultural adaptation of self-reported measures [5]. With the permission of the original author, two translators translated the SDQ into Japanese and a native English language speaker reverse-translated it into English. We sent the back translation to the original author for proofreading, following which permission to use the complete SDQ-J was granted. Because of the difference in the meal cultures, we made certain revisions in the questionnaire like "a cracker" was changed to "a rice cracker" and "pureed food" to "mashed food." All patients answered the SDQ-J without being supervised by the assessors before VF.

Videofluoroscopy

During VF, the patients were seated in the same posture in which they ate their everyday meals, and fluoroscopy was performed from the side. The investigator used a syringe to inject a twofold dilution of 110% w/v liquid barium into the patient's oral cavity and gave the patient the signal to start swallowing. Patients who experienced wearing-off were tested during the "on" state. The patient's swallowing movements were recorded on DVD at 30 frames/s and evaluated for aspiration by an assessor after the test. In order to confirm the reliability of the evaluation of VF results, the same assessor re-evaluated thirty-five VF results and another evaluated same VF results independently. None of the assessors evaluating the VF results was notified of the findings of the SDQ-J.

Statistical analysis

We compared the Hoehn–Yahr (H&Y) stage, sex, and age of the patients with aspiration with that of the patients without aspiration using Mann–Whitney U test. The inter-rater and intra-rater reliability of the evaluation of VF were tested by κ coefficient. Receiver operating characteristic (ROC) analysis was used to determine the cutoff point for the total score of the SDQ-J [6]. We compared SDQ-J findings with aspiration status during VF using the Fisher's exact test. Values of $P < 0.05$ were regarded as significant, and IBM SPSS® (ver. 18.0) statistical software was used for all analyses.

Results

None of the subjects had difficulty comprehending the questionnaire or asked questions about its contents. Cronbach's alpha coefficient for the 15 questions of the SDQ-J was 0.84. With VF, 9 patients (14.8%) aspirated liquid and 52 patients did not aspirate (Table 1). The patients with aspiration had a significantly more severe H&Y stage than those who did not ($P = 0.01$). No significant differences were observed in terms of age and sex. Evaluation of aspiration during VF was highly consistent, with significant internal consistency (κ coefficient 1.00), and consistency between assessors (κ coefficient 0.91, 95% confidence interval (CI) 0.88–0.94).